

Real-time Locally Optimal Schedule for Electric Vehicle Load via Diversity-maximization NSGA-II

Hongqian Wei, Jun Liang, Chuanyue Li, and Youtong Zhang

Abstract—As distributed energy storage equipments, electric vehicles (EVs) have great potential for applications in power systems. Meanwhile, reasonable optimization of the charging time of EVs can reduce the users' expense. Thus, the schedule of the EV load requires multi-objective optimization. A diversity-maximization non-dominated sorting genetic algorithm (DM-NSGA)-II is developed to perform multi-objective optimization by considering the power load profile, the users' charging cost, and battery degradation. Furthermore, a real-time locally optimal schedule is adopted by utilizing a flexible time scale. The case study illustrates that the proposed DM-NSGA-II can prevent being trapped in a relatively limited region so as to diversify the optimal results and provide trade-off solutions to decision makers. The simulation analysis shows that the variable time scale can continuously involve the present EVs in the real-time optimization rather than rely on the forecasting data. The schedule of the EV load is more practical without the loss of accuracy.

Index Terms—Electric vehicle (EV), locally optimal schedule, multi-objective optimization, diversity maximization, genetic algorithm.

NOMENCLATURE

$\alpha_E(y)$	Diversity measure of y
γ_1	Lower limitation of state of charge (SOC)
γ_2	Upper limitation of SOC
ω_i	Weight sum coefficient
Φ^{pwr}	Objective of power load
Φ_k^{ch}	Objective of charging cost for electric vehicle (EV) k
Φ^{bat}	Objective of battery degradation
η_{ch}	Charging efficiency
η_{dch}	Discharging efficiency

Δ_{ie}	Scaling coefficient
CF	Capacity fade at the end of life
C_{lab}	Labor cost for battery displacement
C_k^{bat}	Charging cost per kWh for EV k
CI	Convergence index
d	Cost intercept of linear battery degradation
DOD	Depth of discharge (DOD) of battery at the end of life
E	Subset of Pareto optimality
E_k^{cap}	Battery capacity for EV k
E_k^{dch}	Total energy discharged for EV k
E_k^{ini}	Initial energy of EV k
F_i^M, F_i^m	The maximum and minimum values of objective i
$F_{i,ini}^M, F_{i,cur}^m, F_{i,end}^m$	Initial, current, and final minimal values of objective i in iteration
IGD	Inverted generational distance
K	Charging urgency coefficient of EV
L_c	Battery life cycle at specific DOD
m	Cost slope of linear battery degradation
$M^{(i)}$	Ongoing EV set at time slot i
n_{pop}	Number of individuals in population
n_{gen}	Number of generations
n_{gen}^{max}	The maximum number of generations
P	Pareto frontier
P_i	Ponits in pareto frontier
P_{avg}	Average load demand
P_{peak}	Peak power of power grid
P_{total}	Total power of power grid
P_{max}	The maximum charging power
P_{res}^t	Base load of residential region at time slot t
P_{allow}	Allowance power of power system
P_{peak}^t	Allowance peak charging power at time slot t
$P_{k,veh}^t$	Charging power for EV k at time slot t
$P(x)_{sys}^t$	Total system load at time slot t
$Q^{(j)}$	Charging duration time set for EV k at time slot j

Manuscript received: February 20, 2020; accepted: August 10, 2020. Date of CrossCheck: August 10, 2020. Date of online publication: November 26, 2020.

This work was supported by Chinese Scholarship Council (No. 201906030036) and in part by National Academician Workstation Project (No. 20180525YX002).

This article is distributed under the terms of the Creative Commons Attribution 4.0 International License (<http://creativecommons.org/licenses/by/4.0/>).

H. Wei and Y. Zhang (corresponding author) are with the Low Emission Vehicle (Beijing Key Lab) Research Laboratory, School of Mechanical Engineering, Beijing Institute of Technology, Beijing 100081, China (e-mail: 3120170277@bit.edu.cn; youtong@bit.edu.cn).

J. Liang and C. Li are with the School of Engineering, Cardiff University, Cardiff, CF24 3AA, U.K. (e-mail: LiangJ1@cardiff.ac.uk; LiC9@cardiff.ac.uk).

DOI: 10.35833/MPCE.2020.000093



$RTP(t)$	Real-time price (RTP) at time slot t
S	Data solutions in testing algorithms
S_i	Points in testing algorithms
S_{des}	Desired charging demand
SOC_i^{avg}	Average SOC at time slot t
SOC_i^{cur}	Current SOC at time slot t
t_k^{cur}	Current time for EV k
t_k^{begin}	Plug-in time for EV k
t_k^{end}	Plug-out time for EV k
t_{min}	Shortest charging time
$W^{(i)}$	Specific time window
X	Decision variable set
$x_{ch,k}^t$	Charging power for EV k at time t
$x_{dch,k}^t$	Discharging power for EV k at time t
Y	Pareto optimality
$y^{(i)}$	Objective function i
$y_e^{(i)}$	Objective function i in Pareto subset E

I. INTRODUCTION

TRANSPORTATION is being electrified significantly to meet the goals of decarbonation and low emission. The replacement of internal combustion vehicles with electric vehicles (EVs) plays an important role in electrification [1]. The increase in charging demand from the extensive EVs poses new challenges to the existing distribution system [2]-[4]. References [5] and [6] illustrate that the integration of unordered EV into the power system can damage the grid operation. However, vehicle-to-grid (V2G) technology has been proposed as a cost-effective solution to make full use of the existing network. In general, EVs with V2G are treated as a distributed storage system to support the power grid in terms of reducing the peak demand and compensating the intermittent renewable energy sources [7].

In the application of V2G, reasonable charging or discharging of EVs can benefit multiple parties such as power systems or EV users [8]-[13]. The dispatching of the EV load can serve the power system such as frequency regulation [8]-[10], power load reservation [11], and the reduction of financial expenditure for grid operators [12], [13]. Meanwhile, the electricity-price-oriented charging strategy can reduce the users' charging costs [14], [15]. Cooperative optimization of the charging load can serve the power system and users simultaneously [16]-[18]. Thus, multi-objective optimization approaches deserve more attention because they are concerned with the accuracy and diversity of the optimal results. Some typical linear sum-weighted methods are used to co-optimize multiple objectives. For instance, a weighted sum model of four objectives concerned with grid operation and the users' satisfaction has been constructed by using the particle swarm optimization (PSO) [19]. The adaptive weighted-sum approach has also been utilized [20] to present a dynamic pricing framework for the EV load to co-optimize the power load profile and the profitability of the grid

operator. These approaches convert multiple objectives to a single one by a linear weighted sum, which benefits convex optimization but fails to deal with conflicting objectives such as power load regulation versus the users' charging cost.

Unlike the above approaches which redesign the optimal scheme, multi-objective evolutionary algorithms (MOEAs) such as the nondominated sorting genetic algorithm (NSGA), PSO [21], and the decomposition algorithm (DA) [16], [22], can deal with complex constraints and conflicting objectives. Accelerated PSO has been utilized to solve the multi-objective optimization problem regarding EV user and benefits of grid operator [23]. A stochastic EV model has been introduced to simulate the traveling behavior and activity pattern in real time. EV penetration for capacity expansion has been evaluated to guarantee a lower charging price, traveling plan, and off-peak energy usage. Furthermore, in [24], the electricity variation and stochastic user behavior are analyzed based on real-time forecasting of the EV load. Global optimization has been improved by utilizing a nonlinear autoregressive neural network with exogenous inputs and a time-series-based forecasting approach. Multi-objective optimization based on MOEAs cannot usually obtain a single optimal solution, but it can obtain a set of trade-off solutions that cannot dominate each other in the entire solution space, i.e., the Pareto frontier. Therefore, the solutions to the Pareto frontier reflect the degree of benefit between different objectives. Thus, the decision maker can specify one solution after weighing the benefits and drawbacks. Specifically, the augmented-constraint DA approach can be used to combine the benefits from battery degradation, users' charging cost, and valley filling of the power system [22]. Weight aggregation (WA) PSO has been used to optimize the power load demand and financial investment [25]. MOEAs based on the game-theoretic algorithm have been used to optimize the energy consumption and power load profile in an autonomous and distributed incentive-based energy consumption strategy [26]. MOEAs in the dispatching of EV load has laid the groundwork for the research on how to find trade-off solutions to reshape the power load profile and minimize the users' charging cost simultaneously. Nevertheless, the application of the original MOEAs cannot reach an effective Pareto frontier because the solutions are easily trapped in the local optima in the iteration, especially when solving problems with high-dimensional constraints [27]. To address the above issues, a novel diversity maximization (DM) approach has been embedded into the traditional NSGA-II algorithm to schedule EV charging load in this paper.

Another key concern is the time scale of the optimization, because it determines the accuracy of results and the available EV dispatching capability. Normal optimization is executed in a day-ahead way in which the EV information is stimulated based on the historical data or the Monte Carlo approach [22], [28], [29]. However, the schedule of EV charging in this way shows a low capacity to cope with the random arrivals of EVs and a lower response to the power load fluctuation. Thus, a real-time two-level fuzzy-logic control strategy has been implemented to improve the load re-

sponse with the participation of V2G [29]. Similarly, the demand response has been considered in a real-time EV charging program for parking stations [30]. These real-time schedules have a common feature, i.e., they all address the optimization in the fixed 24-hour period, i.e., a globally optimal schedule. However, the globally optimal schedule is impractical because the accurate power load is required and the future charging information of EVs is unknown. A sliding window has been applied to shorten the optimization period by considering the users' economic expenditure [31]. Thus, in this paper, the time scale is adjustable, and the charging strategy is executed at every time slot, which provides the insight into the locally optimal schedule. An alterable time scale used in multi-objective optimization is determined by the final plug-out time of ongoing EVs at the current time. Specifically, the defined time scale only covers the available EVs, and EVs that arrive at the next time slot are not considered at the current time slot. By continuously executing the charging strategy at every time slot, the charging power of EVs in an entire day can be obtained. The contributions of this paper are as follows.

1) A multi-objective optimization for scheduling the charging load of EVs with a V2G function is solved considering the power load profile, users' cost, and battery degradation. To solve this nonconvex problem and prevent the solutions from being trapped in local optima, a novel DM-NSGA-II algorithm is proposed. The diversity measure is utilized to initialize the population group in NSGA for preprocessing the initial data.

2) A locally optimal schedule with an alterable time scale is utilized. By executing real-time dispatching at every time slot, the strategy has the advantage of coping with a large population of EVs and their random arrivals. The perfor-

mance of the locally optimal schedule is fairly close to that of the globally optimal schedule. However, this approach shows more practical significance for the promotion of V2G technology.

II. EV SCHEDULE ARCHITECTURE AND OPTIMIZATION PERIOD

Figure 1 shows an architecture of charging station and the illustration of the proposed schedule, where F_1 and F_2 are objectives 1 and 2, respectively. The control center receives vehicle profile information and vehicle demand information, which include the battery capacity, initial or target state of charge (SOC), and plug-in and plug-out time, from the EV supply equipment to form the EV-tuple. Meanwhile, it also acquires the base load and real-time price (RTP) from the power system to form the load-tuple. Afterward, the EV-tuple and load-tuple are transmitted to the optimizer. The optimizer identifies the objectives, i.e., power load profile and users' charging cost, defines the time scale of the optimization, and finally executes the multi-objective optimization to obtain the optimal charging power of EVs. Finally, as the dispatching command, the charging power is transferred into every charging pipe in the EV supply equipment. Specifically, the structure of the optimizer is expressed in the description of the optimizer. EVs available at the current time slot are used to define the time scale. Then, multi-objective optimization is processed to form the trade-off solutions. Decision makers can select one solution from these optimal solutions by considering its impact on the power system and EV users. The charging power of EVs is sent to EV supply equipment. Customers are also informed of the charging cost and the cost of battery degradation. In summary, the control center takes responsibility for implementing the optimization and dispatching of the EV load.

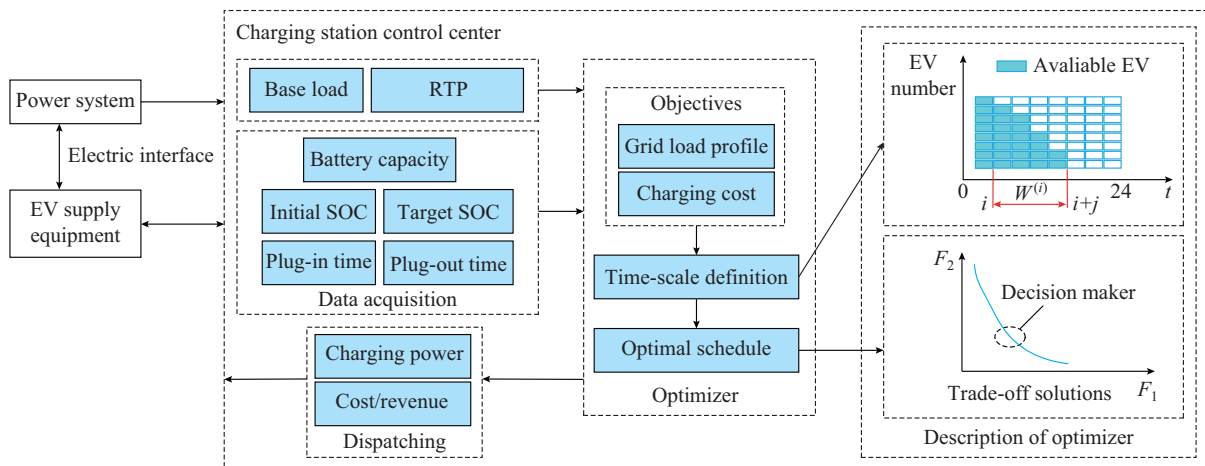


Fig. 1. Architecture of charging station and illustration of proposed schedule.

The time scale of the optimization shows the importance of the precision of solutions and the practical application. In a globally optimal schedule, the time scale is normally given in a fixed time scale of 24 hours based on the global knowledge of the forecasting base load and EV information. Thus, the optimization provides global solutions in a day. However, the locally optimal schedule applies a variable time scale

to optimize the EV load at every time slot. Since the information about EVs in the future is unknown, the definition of the time scale at the current time slot is established using only the available EVs in the parking lot at the current time slot, as shown in Fig. 2. The definitions of the time scale $W^{(i)}$ and the set of available EVs $M^{(i)}$ are as follows. $W^{(i)}$ and $M^{(i)}$ are updated at the beginning of time slot i .

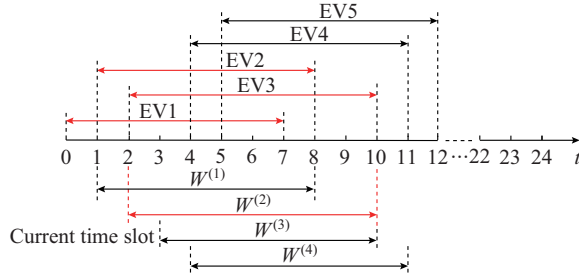


Fig. 2. Varying charging and optimization window.

If the charging period covers t_k^{cur} , exactly satisfying both $t_k^{begin} \leq t_k^{cur}$ and $t_k^{end} > t_k^{cur}$, the EV k belongs to the available EV set $M^{(i)}$. However, the start-time of $W^{(i)}$ is always set to be t_k^{cur} , and its end-time is determined by $\max(t_k^{end} | k \in M^{(i)})$. As shown in Fig. 2, for the time slot $i=2$, EV1 and EV2 are charged for a while, and EV3 is starting to charge, so they all satisfy the conditions $t_k^{begin} \leq t_k^{cur}$ and $t_k^{end} > t_k^{cur}$. And they are allocated into the EV set $M^{(2)}$, denoting $M^{(2)} = \{EV1, EV2, EV3\}$. In terms of time scale $W^{(2)}$, among the ongoing EVs in $M^{(2)}$, EV3 charges longer until 10 am. Accordingly, the time scale is given as $W^{(2)} = \{\text{time slot } 2:10\}$. For each time slot, $W^{(i)}$ and $M^{(i)}$ are updated consecutively. Therefore, the optimizer can perform the real-time multi-objective optimization at the start of the time slot i . With the optimization iteration, the EV load is optimized in an orderly manner, and the command of charging power is transmitted to the EV supply equipment. Thus, in an entire day, the schedule of EV load can be achieved.

III. PROBLEM FORMULATION

A. Objective

In this sub-section, the multi-objective optimization of the EV load is formulated, and two objective functions corresponding to the power load profile and the total costs of EV users are constructed from the perspectives of power system operators and users, respectively.

1) Power load profile: from the perspective of grid operators, power load fluctuation in one day is the primary concern. Disordered charging of EVs drives up the peak load, blocks the power source, and incurs network stress. Therefore, it is necessary to minimize the overall load variance [32] so as to coordinate the EV charging load in a specified time window. Normally, coordinated load schedule of EVs can reduce the deviation between the instantaneous and the average load and can act as a peak-shaving and valley-filling in the global view. Thus, the first objective of reshaping the power load profile is defined as:

$$\arg \min_x F_1(x) = \Phi^{pwr} \quad (1)$$

$$\Phi^{pwr} = \text{var}(P_{total}) = \sum_{t \in W^{(i)}} (P(x)_{sys}^t - P_{avg})^2 \quad (2)$$

$$P(x)_{sys}^t = P_{res}^t + \sum_{k \in M^{(i)}} P_{k,veh}^t \Delta t \quad (3)$$

$$P_{k,veh}^t = x_{ch,k}^t / \eta_{ch} - x_{dch,k}^t \eta_{dch} \quad (4)$$

The objective function is programmed in $W^{(i)}$. However, to fully flatten the total daily peak load, the average load P_{avg}

is obtained by traversing the entire time granularity in one day.

2) Users' cost and revenue model: from the users' perspective, charging cost is the most important concern. The time-of-use (TOU) electricity tariff is widely used in most utilities as an incentive to motivate users to charge at the power load valley and discharge batteries back to the power system at the load peak. V2G activities can help EV owners earn the revenue to some extent, which also has great significance in reducing power peak demand for the power system. RTP based on three-tier tariff is utilized to formulate the charging costs as:

$$\Phi_k^{ch} = \sum_{t \in W^{(i)}} P_{k,veh}^t \Delta t \cdot RTP(t) \quad (5)$$

Although the participation in the V2G can bring certain returns to users, cyclic charging and discharging of the battery can degrade the battery lifetime adversely and also incur extra costs. Generally, battery degradation is intensively distributed in capacity fade, which is composed of two crucial components [33], [34]: SOC-related degradation $\Phi_{k,t}^{SOC}$ and depth of discharge (DOD) degradation $\Phi_{k,t}^{DOD}$. The mathematical formulation of the two components is defined as:

$$\Phi_{k,t}^{SOC} = C_k^{bat} (m \cdot SOC_t^{avg} - d) / (8760 \cdot CF \cdot L_c) \quad (6)$$

$$\Phi_{k,t}^{DOD} = (C_k^{bat} E_k^{cap} + C_{lab}) E_k^{dch} / (L_c E_k^{cap} \cdot DOD) \quad (7)$$

The total cost incurred by battery degradation is therefore expressed as:

$$\Phi_k^{bat} = \sum_{t \in W^{(i)}} (\Phi_{k,t}^{SOC} + \Phi_{k,t}^{DOD}) \quad k \in M^{(i)} \quad (8)$$

It has been proved [22] that battery degradation negatively correlates to the users' revenue during V2G. Thus, the objective function from the users' perspective is formulated with a simple summation as:

$$\arg \min_x F_2(x) = \sum_{k \in M^{(i)}} (\Phi_k^{ch} + \Phi_k^{bat}) \quad (9)$$

B. Constraint

This optimization problem is constrained by grid operators and EV battery characteristics. Specifically, the objective functions must be subjected to the charging power of the charger, power load peak constraints, the energy requirements of EV, and battery SOC constraints. For each k and time slot i , the following constraints are shown as:

$$P_{min} < P_{k,veh}^t < P_{max} \quad (10)$$

$$\sum_{k \in M^{(i)}} P_{k,veh}^t \Delta t \leq P_{peak} - P_{sys}^t \quad (11)$$

$$E_k^{ini} + \sum_{t \in Q^{(i)}} P_{k,veh}^t \Delta t \geq \gamma_1 E_k^{cap} \quad (12)$$

$$E_k^{ini} + \sum_{t \in Q^{(i)}} P_{k,veh}^t \Delta t \geq \gamma_2 E_k^{cap} \quad (13)$$

Constraints (10) and (11) define the charging or discharging power limitation and total grid peak load constraints for all EVs, respectively. Constraint (12) demonstrates the energy requirement for one EV during one entire charging period. Constraint (13) ensures that the battery is not overcharged or over-discharged to maintain the battery lifetime.

IV. IMPLEMENTATION OF MULTI-OBJECTIVE OPTIMIZATION

Unlike single-objective optimization aiming to seek an optimal solution, multi-objective optimization tries to find a set of solutions that are called as Pareto frontier. NSGA-II algorithm is used to obtain Pareto frontier, which formulates a set of particles for continuously nondominated sorting, crossover, and mutation [35]. Furthermore, to address the defect of local optima and poor convergence ability in traditional NSGA-II algorithm, the DM approach is introduced to maximize the solution diversity.

A. DM

DM approach seeks the optimal solution for multi-objective optimization by pursuing all more diverse solutions. With a subset $E \subset Y$, a solution diversity measure $\alpha_E(y)$ of one available particle is defined as:

$$\alpha_E(y) = \max_{y_e \in E} \left(\min_{1 \leq i \leq k} \frac{y^{(i)} - y_e^{(i)}}{\Delta_{ie}} \right) \quad (14)$$

$$\Delta_{ie} = \max_{y_e \in E} y_e^{(i)} - \min_{y_e \in E} y_e^{(i)} \quad (15)$$

Δ_{ie} is used to normalize different objectives. According to the definition of solution diversity, the logic rule description is presented in Table I.

TABLE I
RULES OF DIVERSITY RELATIONS

Constraint	Rule
$\alpha_E(y) > 0$	y_e is dominated by $y_e \in E$
$\alpha_E(y) < 0$	y is not dominated by $y_e \in E$
$\alpha_E(y) = 0$	$y_e \leq y$ for some y_e and $y_e^{(i)} = y^{(i)}$ for some i
$\alpha_1(y) < \alpha_E(y)$	y is not dominated by y_1 for some $y_1 \in Y$

As shown in Fig. 3, it is supposed that $\Delta_{ie} = 1$ and that $Y = \{y_1, y_2, y_3, y_{e1}, y_{e2}\}$ is the objective set, $E = \{y_{e1}, y_{e2}\}$ is the subset of Y , and the Pareto frontier $Y_{PF} = \{y_1, y_3, y_{e1}, y_{e2}\}$. Then, the diversity measure of y_1 and y_2 is represented as:

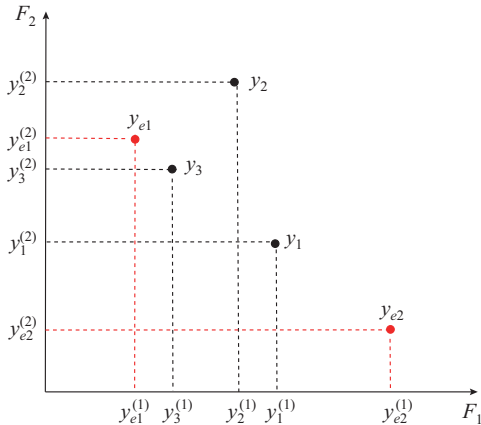


Fig. 3. Illustration of solution diversity measure.

$$\alpha_E(y_1) = \max \left(\min (y_1^{(1)} - y_{e1}^{(1)}, y_1^{(2)} - y_{e1}^{(2)}), \min (y_1^{(1)} - y_{e2}^{(1)}, y_1^{(2)} - y_{e2}^{(2)}) \right) \quad (16)$$

$$\alpha_E(y_2) = \max \left(\min (y_2^{(1)} - y_{e1}^{(1)}, y_2^{(2)} - y_{e1}^{(2)}), \min (y_2^{(1)} - y_{e2}^{(1)}, y_2^{(2)} - y_{e2}^{(2)}) \right) \quad (17)$$

According to (16), $\alpha_E(y_1) = \max (y_1^{(2)} - y_{e1}^{(2)}, y_1^{(1)} - y_{e2}^{(1)})$, both $y_1^{(2)} - y_{e1}^{(2)} < 0$ and $y_1^{(1)} - y_{e2}^{(1)} < 0$ result in $\alpha_E(y_1) < 0$, and the denoting point y_1 is not dominated by other points in subset E . Similarly, $\alpha_E(y_2) = \max (y_2^{(2)} - y_{e1}^{(2)}, y_2^{(1)} - y_{e2}^{(1)}) = y_2^{(1)} - y_{e2}^{(1)} > 0$ means that point y_2 is dominated by at least one point in set E such as point y_{e1} .

However, considering the diversity of points in set E , $\alpha_E(y_1) = y_1^{(2)} - y_{e1}^{(2)}$ and $\alpha_E(y_3) = y_3^{(2)} - y_{e1}^{(2)}$, $\alpha_E(y_3) > \alpha_E(y_1)$, since y_1 is far away from y_{e1} over y_3 . Therefore, point y_1 is defined as a more diverse solution than point y_3 . The DM approach finds more diverse solutions such as point y_1 so as to construct the entire initial population before implementing NSGA-II. The DM approach starting with the empty E is presented in (18)-(20).

$$\min Z = \sum_{i=1}^K \omega_i y^{(i)} \quad (18)$$

$$\min Z = \min_X \left(\alpha_E(y), \sum_{i=1}^K \omega_i y^{(i)} \right) \quad (19)$$

s.t.

$$\alpha_E(y) = \max_{y_e \in E} \left(\min_{1 \leq i \leq k} \frac{y^{(i)} - y_e^{(i)}}{\Delta_{ie}} \right) \quad (20)$$

Concretely, the DM approach is executed as follows.

Step 1: solve (18) with any $\omega_i > 0$ and obtain the optimal solution y_m . Set $E = \{y_m\}$ and select a small $\zeta \geq 0$, where ζ is used to decide the terminal condition of the iteration.

Step 2: solve the problem in (19) and continuously obtain the optimal solution y_m^* .

Step 3: execute the decision. If $\alpha_E(y_m^*) < -\zeta$, update $E = E \cup y_m^*$, and go back to *Step 1*. Otherwise, stop the iteration.

Step 4: obtain the entire feasible set E with y_m^* .

For every iteration, one feasible solution y_m^* is added to feasible set E and the absolute value of $\alpha_E(y_m^*)$ is smaller than its value in the last iteration. Therefore, a small value ζ is used to decide when to terminate the iteration after obtaining sufficient solutions in feasible set E .

B. DM-NSGA-II

In this sub-section, DM-NSGA-II and its flowchart are described. The main steps are as follows.

1) DM Approach

Obtain the base load, RTP, ongoing EV set $M^{(0)}$ and its configuration information, and system constraints. Decide the parameters in the genetic algorithm such as n_{pop} , n_{gen}^{max} , crossover, and mutation rate. Execute the DM algorithm to generate initial particles and then transmit the parameters and initial particles to NSGA-II.

2) Nondominated Sorting and Crowding Distance

Classify the particles and confirm their rank, which evaluates the distance of particles spreading along the fronts. Sort the individuals according to the rank to which they belong. Calculate the crowding distance among particles.

3) Iterative Process

Repeat the following loop before n_{gen} reaches the maxi-

imum number of generations n_{gen}^{max} .

1) Selection: a tournament game would select two particles to participate in the crossover and mutation. A particle with a high priority rank or a larger crowding distance of the same rank would be selected to take part in the tournament game.

2) Crossover and mutation: simulated binary crossover and polynomial mutation are adopted to generate the temporary offspring population.

3) Recombination: recombine the parent chromosome and offspring chromosome to generate a temporary population with $2n_{pop}$ particles.

4) Nondominated sorting and crowd distance: the particles in the temporary population are classified again based on the nondominated relationship and crowding distance.

5) Generation of a new population (elite selection): a new population is obtained by selecting the best half particles with high priority rank and diversity from the temporary population.

4) Results

The particles after iterations make up the entire Pareto frontier, which contains particles with the highest priority rank. Every particle denotes a specific decision variable set containing the charging power of all ongoing EVs and current objective values.

V. RESULTS AND DISCUSSION

One typical base load of a parking lot in Beijing, China and the RTP tariff in Table II are used to simulate and evaluate the proposed algorithm. Without the loss of generality, time granularity is set to be 1 hour, and the entire scheduling time is 24 hours by consecutively performing local optimization. An EV with a time-space characteristic is regarded as a distributed load, and its control focuses on the charging or discharging power in the dispatching period.

TABLE II
TARIFF PRICE OF ELECTRICITY

Price (\$)	Time slot
0.2578	10:00-15:00, 18:00-21:00
0.2136	7:00-10:00, 15:00-18:00, 21:00-23:00
0.1707	23:00-7:00

A. Simulation Setting

The competing objective includes the minimization of the users' charging cost. Corresponding to the two objectives, the cost functions are defined in (1) and (9), respectively. In this paper, the battery capacity is 28 kWh, the EV charging power is limited to 5 kW, and the EV battery should be at least 90% of SOC to ensure the normal operation of EVs. Furthermore, excessive discharging of the battery significantly affects the battery health and even reduces its life. Therefore, when the SOC value of the battery is lower than a certain value, the self-protection program of the battery management system is initiated [36], [37]. Therefore, the batteries discharge no less than 10% of SOC to avoid being over-discharged.

To encourage the orderly charging of EVs, charging stations can sign a price stimulation agreement with EV users.

If the users participate in the schedule plan, they can enjoy lower electricity prices and sell excess electricity to the power system at higher prices, thus maximizing the revenue. Furthermore, according to different charging demands, a charging priority mechanism is introduced to measure the urgency of the charging process. The specific implementation is as follows.

The charging demand is defined as:

$$S_{des} = (1 - SOC_i^{cur}) E_k^{cap} \quad (21)$$

Considering that, after EV connection, if the battery is fully charged with the maximum power, the consumed time is the shortest.

$$t_{min} = \frac{S_{des}}{P_{max}} \quad (22)$$

Then, the charging urgency coefficient of EV can be expressed as:

$$K = \frac{t_k^{end} - t_k^{begin}}{t_{min}} \quad (23)$$

If $K > 1.5$, EV has enough time to participate in V2G, and the proposed EV scheduling strategy can be executed. If $K \leq 1.5$, EV needs to leave in a short period of time, so it is not suitable to feedback extra electric energy to the power system, and the battery should be charged with the maximum charging power. The implementation flowchart of charging is shown in Fig. 4, and the specific charging priority criteria are listed in Table III.

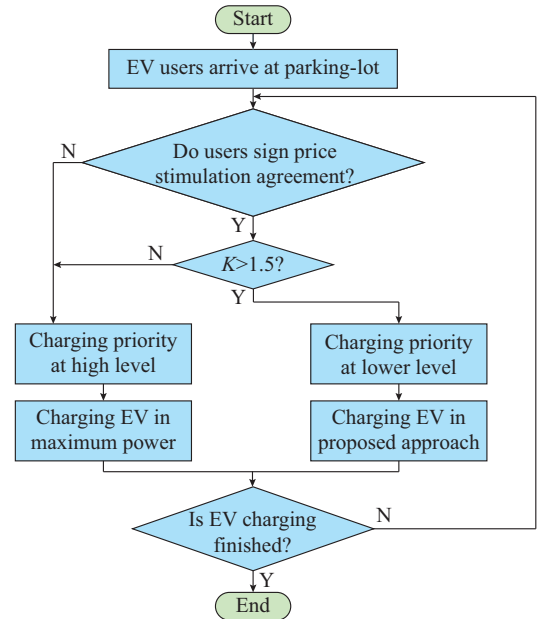


Fig. 4. Implementation flowchart of charging.

TABLE III
CHARGING PRIORITY CRITERIA

Charging priority	Does EV participate in schedule plan?	$K > 1.5?$	Charging effect
1	Yes	Yes	Executing proposed strategy
		No	Charging in P_{max}
0	No		Charging in P_{max}

ILOG CPLEX tool package is utilized to implement the single-objective optimization and initialize the particles. MATLAB is used to implement NSGA-II in an Intel i7 1.80 GHz PC with 8 GB of RAM running Windows 10 and visual C++ 6.0.

B. Performance Evaluation of Locally Optimal Schedule

The performance of the local schedule is shown in Fig. 5, and the corresponding cases are defined as follows.

1) Case 0: uncoordinated EV charging. In this case, batteries are charged with rated charging power once the EV arrives, regardless of the EV departure information and the ability of V2G.

2) Case 1: power system operator focused. Power load fluctuation is minimized, and better peak-shaving and valley-filling are achieved with the participation of EVs.

3) Case 2: user focused. Charging cost and battery degradation cost are minimized.

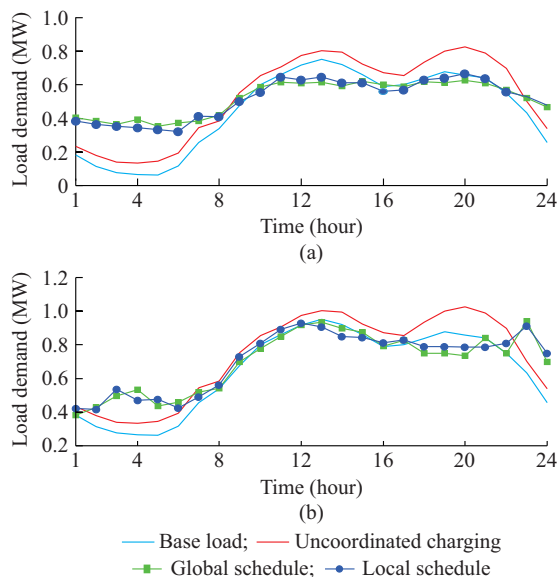


Fig. 5. Comparison of global and local schedule for individual objective. (a) Case 1. (b) Case 2.

As shown in Fig. 5(a), uncoordinated charging drives up the power load uniformly at any time slot, apparently resulting in a sharp increase in the peak demand during the noon (12:00-2:00 pm) and evening (6:00-9:00 pm). The curves of case 1 show that, with the participation of uncoordinated charging, the global and local optimal schedules can reshape the load profile and efficiently decrease the peak-to-valley difference. Compared with the global schedule, the fluctuation of the load in the locally optimal schedule is more distinct. However, experimental data show that this only accounts for 8.5% of deviation over the global schedule in power variance. Considering the unknown information on the future base load and EV arrivals, the local optimal schedule is more practical for load dispatching without much loss of accuracy.

Figure 5(b) shows the power load curve when implementing the second objective optimization. The charging load curve varies with RTP, but results in a severe peak around

midnight, especially at 11:00 pm. By viewing the time slot from 4:00 pm to 8:00 pm, it can be seen that the deviation of the power load profile is between the existing global and local schedules. In the local optimal schedule, the upcoming EVs arriving later than the current time slot are not considered.

C. Comparison of DM-NSGA-II Versus Existing Approaches

In the genetic algorithm, a particle denotes one individual decision variable set $X = [x_1, x_2, \dots, x_M]$, and it has a dimension of $|M_i| \times |W_i|$, where $|M_i|$ is the EV count in the current W_i . For this case, $i=19$; $|M_i|=112$; the population size is 85; the iteration count is 1500; and the distribution indexes for crossover and mutation are both 5. According to the result of single-objective optimization, the minimal F_1^m and F_2^m are 624212.7 (kW)^2 and $\$252.43$, respectively, which are considered as evaluation criteria for extremely optimal results.

1) Development of Initial Particles in DM

The development of initial particles is shown in Fig. 6, in which the particle count and diversity measure α are presented. The figure presents six stages of the generation of the initial particles in the DM approach. The representative points are also presented, starting with two edges and the middle point. There is one generation point in each iteration based on the DM rules. Five points are generated in Fig. 6(b), and the distance between particles is kept as large as possible according to the definition of the diversity measure. As the number of particles increases, the absolute value of α decreases relatively quickly to a small value close to zero in Fig. 6(f), when all initial particles are generated. It means that the solutions are very close to the final Pareto frontier. Considering the development of initialization in DM, it can be seen that the particles are generated continuously, keeping each solution more diverse with $\alpha=-0.78$ in Fig. 6(a) to the final -0.004 in Fig. 6(f). Figure 6 shows that the acquired particles are equitably distributed around the Pareto frontier.

2) Comparison with Existing Approaches

WA-NSGA-II [23] shows a good ability to obtain particles close to the Pareto frontier. Therefore, it is used to make a comparison with the proposed approach in this paper.

Figure 7(a)-(c) shows the initial positions before implementing NSGA-II, while Fig. 7(d)-(f) show the final Pareto optimum. Figure 7(d) shows that, after a long-term iteration, the original NSGA-II shows a Pareto-like behavior, but the detailed values $F_1^m=682969$, $F_2^m=300.64$ are still far from the Pareto frontier. Additionally, sophisticated constraints and decision variables are severe obstacles for particles.

Compared with Fig. 7(a), the particles in Fig. 7(b) are closer to the Pareto frontier, and the objective values are close to the true optimal values. However, the particles in Fig. 7(e) stop evolving before the population reaches a true Pareto frontier as $F_1^m=636213 \text{ (kW)}^2$ and $F_2^m=284.13 \text{ \$}$. It is evident that the particles are trapped in local optima. In Fig. 7(b), superabundant particles gather in the restricted region at the initial stage. Even if there are nondominated sorting, they are still easily trapped in a small area in the genetic process.

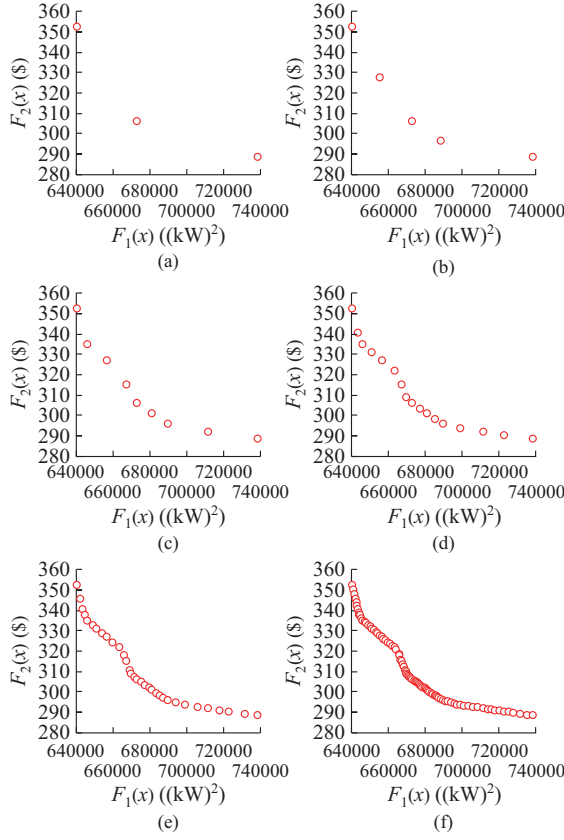


Fig. 6. Development of initial particles using DM approach. (a) 3 solutions ($\alpha=-0.782$). (b) 5 solutions ($\alpha=-0.318$). (c) 9 solutions ($\alpha=-0.169$). (d) 17 solutions ($\alpha=-0.062$). (e) 33 solutions ($\alpha=-0.021$). (f) 85 solutions ($\alpha=-0.004$).

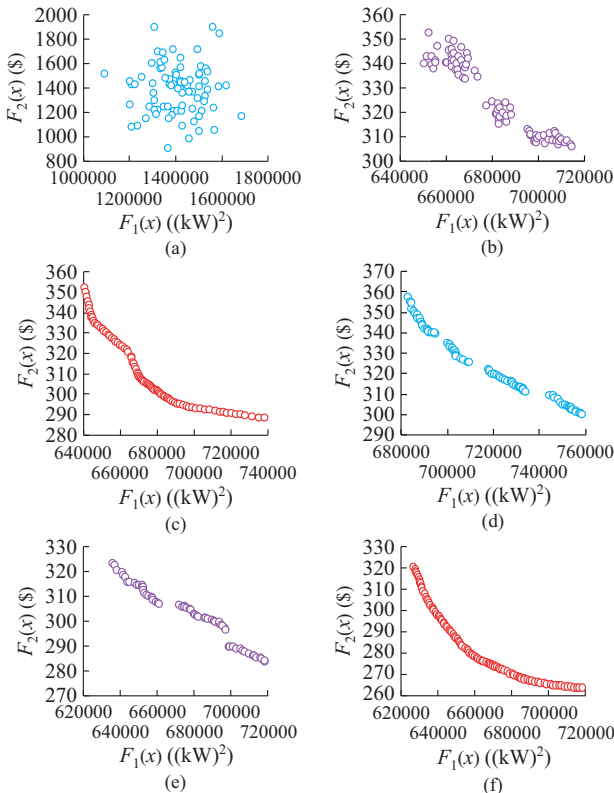


Fig. 7. Experimental results. (a) Random initialization. (b) WA initialization. (c) DM initialization. (d) NSGA-II. (e) WA-NSGA-II. (f) DM-NSGA-II.

3) Comparison of Accuracy and Computation

The accuracy of the optimal results for multi-objective optimization is essential for decision makers. Furthermore, the computation efforts should also be examined by the simulation. The inverted generational distance (IGD) [38] and convergence index (CI) are introduced to evaluate the performance of the optimization approach and computation efforts. The formula of IGD is shown in (24) and (25).

$$IGD = \frac{1}{|P|} DIS_i \quad (24)$$

$$DIS_i = \min_{i=1}^{|S|} \sqrt{\left(\frac{F_1(p_i) - F_1(s_i)}{F_1^M - F_1^m}\right)^2 + \left(\frac{F_2(p_i) - F_2(s_i)}{F_2^M - F_2^m}\right)^2} \quad (25)$$

Equation (25) expresses the normalized distance from the experimental point to its nearest reference point. IGD represents how close the actual Pareto front is to its theoretical values. For instance, the smaller the IGD, the closer the optimized Pareto front to its theoretical solutions.

The true Pareto frontier is not readily available. Therefore, two black lines are constructed where 100 reference dots are evenly selected along the horizontal and vertical segments starting from points A and B, as shown in Fig. 8. To fully eliminate the randomness of the trial, each genetic algorithm runs 10 times, and the statistical results of IGD are shown in Table IV. DM-NSGA-II has the lowest mean IGD, implying that the closest distance to the true Pareto frontier and solutions are more diverse. At the same time, the standard deviation indicates that DM-NSGA-II is more stable in searching for an optimal solution.

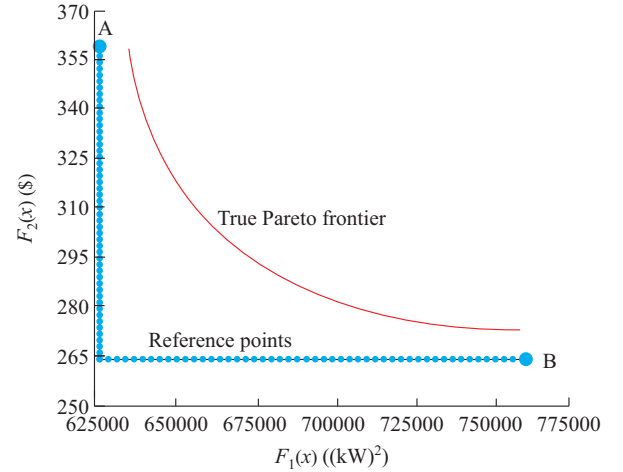


Fig. 8. Selection of reference points in IGD.

TABLE IV
IGD RESULTS FOR THREE ALGORITHMS

Item	IGD		
	NSGA-II	WA-NSGA-II	DM-NSGA-II
Mean	0.6562	0.4426	0.2486
Standard	0.0413	0.0345	0.0292
Maximum	0.7214	0.4938	0.2715
Minimum	0.6001	0.4066	0.2048

Finally, the minimum cost function in the iteration process is exhibited in Table V to describe the iteration characteristics. Specifically, CI denotes the iteration speed and represents the degree to which the data points converge to the final values. The mathematical form is defined as:

$$CI = \frac{|F_{i,cur}^m - F_{i,ini}^m|}{|F_{i,ini}^m - F_{i,end}^m|} \quad (26)$$

TABLE V
CI RESULTS

Iteration	NSGA-II		WA-NSGA-II		DM-NSGA-II	
	F_1 (%)	F_2 (%)	F_1 (%)	F_2 (%)	F_1 (%)	F_2 (%)
50	8.5	6.9	27.2	25.5	25.7	29.8
100	16.2	15.4	45.1	48.2	44.8	49.5
200	54.3	49.7	69.2	74.3	68.3	76.4
300	74.4	72.2	86.0	87.5	85.5	89.2
500	87.2	88.7	94.9	94.6	93.5	95.2
700	92.4	93.7	99.2	97.5	98.1	99.1
900	96.6	97.4	100.0	100.0	100.0	100.0
1200	100.0	100.0	100.0	100.0	100.0	100.0

The genetic algorithm after WA and DM processes can obviously accelerate the iteration compared with the original NSGA-II. After preprocessing WA or DM, the particles can directly start evolving, while the particles with random initialization must be repeatedly sorted and selected before continuing to evolve.

D. Analysis of Optimal Results for Different Objectives

In Section III, the users' charging costs and battery degradations are merged to account for the total charging costs of EV users. In this sub-section, the power load profile in (1), EV charging cost in (5), and the battery degradation in (8) are separated to discuss their contradictions. Figure 9 illustrates the Pareto frontier with the proposed DM-NSGA-II.

1) Battery degradation versus users' charging cost: Fig. 9(a) shows that there is an apparent Pareto relation between battery health and users' charging cost, which means that they are in conflict with each other. To minimize the charging cost and earn extra profit, it is necessary for EV users to sell extra electricity to the power system under high-price conditions. However, (7) presents that frequent charging and discharging will damage the battery life.

2) Power load profile versus users' charging cost: since the curve of minimizing the charging cost distinctly fluctuates following the real-time TOU price, and the objective of the power profile system is to balance the load fluctuation, they are in conflict with each other at some key time slots. Therefore, a certain Pareto relationship is shown in Fig. 9(b).

3) Power load profile versus battery degradation: Fig. 9(c) shows a Pareto behavior between the power load and battery degradation. Meanwhile, they can reach a mutual consistency according to a certain selection criterion.

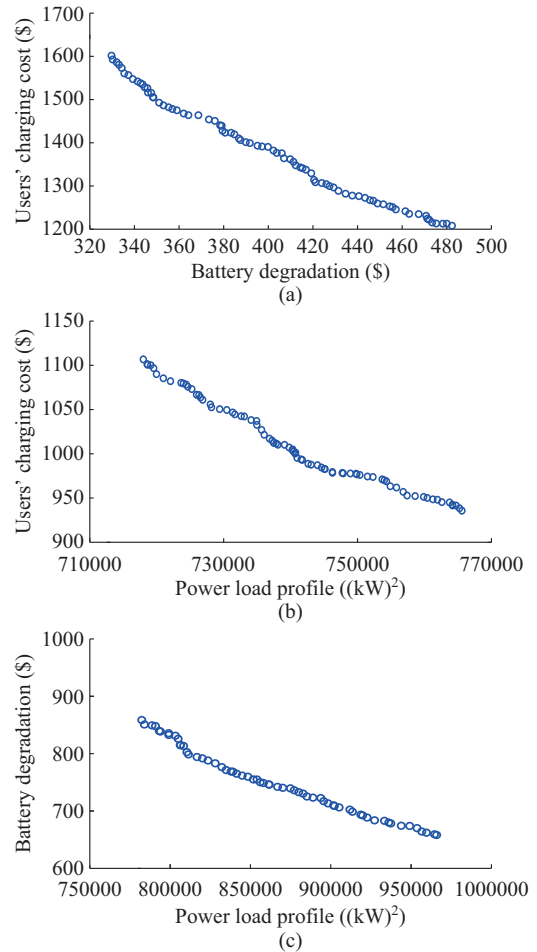


Fig. 9. Pareto frontier. (a) Battery degradation versus users' charging cost. (b) Power load profile versus users' charging cost. (c) Power load profile versus battery degradation.

VI. CONCLUSION

A real-time locally optimal schedule for EV charging load is established by considering the peak-shaving and valley-filling for the power system, user's charging expenditure, and the battery degradation. In the locally optimal schedule, a flexible time scale based on the available EVs at the current time slot is adopted to address the random arrivals of EVs. With continuous optimization at every time slot, the charging power of EVs in an entire day can be obtained. The optimal result of power variance in the locally optimal schedule shows approximately 8.5% of deviation compared with the globally optimal schedule, which is acceptable since the local optimal load schedule would not excessively rely on the EV travel information. However, to solve the problem in the original genetic algorithms where the solutions on the Pareto frontier are not diverse, the proposed DM-NSGA-II is utilized to execute multi-objective optimization. The DM approach can change the initial state of particles and reduce the iteration time. Compared with the original NSGA-II and WA-NSGA-II, the proposed algorithm can effectively reduce at least 43.8% of the inverted generational distance, which reflects a more accurate fitting to the true Pareto frontier.

The diverse solutions using the proposed strategy can provide a more practical and accurate choice for decision makers.

REFERENCES

- [1] M. Amjad, A. Ahmad, M. H. Rehmani *et al.*, "A review of EVs charging: from the perspective of energy optimization, optimization approaches, and charging techniques," *Transportation Research Part D: Transportation and Environment*, vol. 62, pp. 386-417, Jul. 2018.
- [2] R. C. Green, L. Wang, and M. Alam, "The impact of plug-in hybrid electric vehicles on distribution networks: a review and outlook," *Renewable and Sustainable Energy Reviews*, vol. 15, no. 1, pp. 544-553, Jan. 2011.
- [3] R. Mehta, D. Srinivasan, A. Trivedi *et al.*, "Hybrid planning method based on cost-benefit analysis for smart charging of plug-in electric vehicles in distribution systems," *IEEE Transactions on Smart Grid*, vol. 10, no. 1, pp. 523-534, Aug. 2017.
- [4] H. Lin, Y. Liu, Q. Sun *et al.*, "The impact of electric vehicle penetration and charging patterns on the management of energy hub – a multi-agent system simulation," *Applied Energy*, vol. 230, pp.189-206, Nov. 2018.
- [5] S. Habib, M. Khan, F. Abbas *et al.*, "Risk evaluation of distribution networks considering residential load forecasting with stochastic modeling of electric vehicles," *Energy Technology*, vol. 7, no. 7, pp. 191-211, Jul. 2019.
- [6] S. Habib, M. Khan, F. Abbas *et al.*, "A framework for stochastic estimation of electric vehicle charging behavior for risk assessment of distribution networks," *Frontiers in Energy*, vol. 648, no. 5, pp. 1-20, Nov. 2019.
- [7] F. Mwasilu, J. Justo, E. Kim *et al.*, "Electric vehicles and smart grid interaction: a review on vehicle to grid and renewable energy sources integration," *Renewable and Sustainable Energy Reviews*, vol. 34, pp. 501-516, Jun. 2014
- [8] K. Kaur, N. Kumar, and M. Singh, "Coordinated power control of electric vehicles for grid frequency support: MILP-based hierarchical control design," *IEEE Transactions on Smart Grid*, vol. 10, no. 3, pp. 3364-3373, Apr. 2018.
- [9] H. Liu, J. Qi, J. Wang *et al.*, "EV dispatch control for supplementary frequency regulation considering the expectation of EV owners," *IEEE Transactions on Smart Grid*, vol. 9, no. 4, pp. 3763-3772, Dec. 2016.
- [10] X. Chen, K. Leung, A. Lam *et al.*, "Online scheduling for hierarchical vehicle-to-grid system: design, formulation, and algorithm," *IEEE Transactions on Vehicular Technology*, vol. 68, no. 2, pp. 1302-1317, Dec. 2018.
- [11] X. Bai and W. Qiao, "Robust optimization for bidirectional dispatch coordination of large-scale V2G," *IEEE Transactions on Smart Grid*, vol. 6, no. 4, pp. 1944-1954, Feb. 2015.
- [12] C. Shao, X. Wang, X. Wang *et al.*, "Hierarchical charge control of large populations of EVs," *IEEE Transactions on Smart Grid*, vol. 7, no. 2, pp. 1147-1155, Feb. 2015.
- [13] C. Shao, X. Wang, X. Wang *et al.*, "Layered and distributed charge load dispatch of considerable electric vehicles," *IEEE Transactions on Power Systems*, vol. 30, no. 4, pp. 1858-1867, Oct. 2014.
- [14] R. Mehta, D. Srinivasan, A. Khambadkone *et al.*, "Smart charging strategies for optimal integration of plug-in electric vehicles within existing distribution system infrastructure," *IEEE Transactions on Smart Grid*, vol. 9, no. 1, pp. 299-312, Apr. 2018.
- [15] J. Chen, "Electric vehicle charging schedule considering users' charging selection from economics," *IET Generation, Transmission & Distribution*, vol. 13, no. 15, pp. 3388-3396, Apr. 2019.
- [16] I. Martinez, J. Zamora, and P. Eguia, "Energy management of micro renewable energy source and electric vehicles at home level," *Journal of Modern Power Systems and Clean Energy*, vol. 5, no. 6, pp. 979-990, Nov. 2017.
- [17] P. Hou and G. Yang, "Convex optimization of virtual storage system scheduling in market environment," *Journal of Modern Power Systems and Clean Energy*, vol. 7, no. 6, pp. 1744-1748, Nov. 2019.
- [18] L. Wang, S. Sharkh, A. Chipperfield *et al.*, "Dispatch of vehicle-to-grid battery storage using an analytic hierarchy process," *IEEE Transactions on Vehicular Technology*, vol. 66, no. 4, pp. 2952-2965, Jul. 2017.
- [19] J. Yang, L. He, and S. Fu, "An improved PSO-based charging strategy of electric vehicles in electrical distribution grid," *Applied Energy*, vol. 128, pp. 82-92, Sept. 2014.
- [20] C. Luo, Y. Huang, and V. Gupta, "Stochastic dynamic pricing for EV charging stations with renewable integration and energy storage," *IEEE Transactions on Smart Grid*, vol. 9, no. 2, pp. 1494-1505, Mar. 2018.
- [21] J. Yang, L. He, and S. Fu, "An improved PSO-based charging strategy of electric vehicles in electrical distribution grid," *Applied Energy*, vol. 128, pp. 82-92, Sept. 2014.
- [22] M. Crow, "Electric vehicle scheduling considering co-optimized customer and system objectives," *IEEE Transactions on Sustainable Energy*, vol. 9, no. 1, pp. 410-419, Aug. 2018.
- [23] F. Abbas, D. Feng, S. Habib *et al.*, "A heuristically optimized comprehensive charging scheme for large-scale EV integration," *International Transactions on Electrical Energy Systems*, vol. 30, no. 5, pp. 12313-12333, May 2019.
- [24] F. Abbas, D. Feng, S. Habib *et al.*, "An improved optimal forecasting algorithm for comprehensive electric vehicle charging allocation," *Energy Technology*, vol. 7, no. 10, pp. 436-457, Oct. 2019.
- [25] Q. Kang, S. Feng, M. Zhou *et al.*, "Optimal load scheduling of plug-in hybrid electric vehicles via weight-aggregation multi-objective evolutionary algorithms," *IEEE Transactions on Intelligent Transportation Systems*, vol. 18, no. 9, pp. 2557-2568, May 2017.
- [26] A. Mohsenian-Rad, V. Wong, J. Jatskevich *et al.*, "Autonomous demand-side management based on game-theoretic energy consumption scheduling for the future smart grid," *IEEE Transactions on Smart Grid*, vol. 1, no. 3, pp. 320-331, Nov. 2010.
- [27] M. Masin and Y. Bukchin, "Diversity maximization approach for multiobjective optimization," *Operations Research*, vol. 56, no. 2, pp. 411-424, Apr. 2008.
- [28] Z. Liu, Q. Wu, K. Ma *et al.*, "Two-stage optimal scheduling of electric vehicle charging based on transactive control," *IEEE Transactions on Smart Grid*, vol. 10, no. 3, pp. 2948-2958, Mar. 2018.
- [29] M. Singh, K. Thirugnanam, P. Kumar *et al.*, "Real-time coordination of electric vehicles to support the grid at the distribution substation level," *IEEE Systems Journal*, vol. 9, no. 3, pp.1000-1010, Sept. 2013.
- [30] L. Yao, W. Lim, and T. Tsai, "A real-time charging scheme for demand response in electric vehicle parking station," *IEEE Transactions on Smart Grid*, vol. 8, no. 1, pp. 52-62, Jun. 2016.
- [31] Y. He, B. Venkatesh, and L. Guan, "Optimal scheduling for charging and discharging of electric vehicles," *IEEE Transactions on Smart Grid*, vol. 3, no. 3, pp. 1095-1105, Jul. 2012.
- [32] X. Chen, K. Leung, A. Lam *et al.*, "Online scheduling for hierarchical vehicle-to-grid system: design, formulation, and algorithm," *IEEE Transactions on Vehicular Technology*, vol. 68, no. 2, pp. 1302-1317, Dec. 2018.
- [33] J. Tan and L. Wang, "Integration of plug-in hybrid electric vehicles into residential distribution grid based on two-layer intelligent optimization," *IEEE Transactions on Smart Grid*, vol. 5, no. 4, pp. 774-1784, Jul. 2014.
- [34] A. Ahmadian, M. Sedghi, B. Mohammadi-ivatloo *et al.*, "Cost-benefit analysis of V2G implementation in distribution networks considering PEVs battery degradation," *IEEE Transactions on Sustainable Energy*, vol. 9, no. 2, pp. 961-970, Nov. 2017.
- [35] K. Deb, A. Pratap, S. Agarwal *et al.*, "A fast and elitist multiobjective genetic algorithm: NSGA-II," *IEEE Transactions on Evolutionary Computation*, vol. 6, no. 2, pp. 182-197, Aug. 2002.
- [36] A. Hoke, A. Brissette, K. Smith *et al.*, "Accounting for lithium-ion battery degradation in electric vehicle charging optimization," *IEEE Journal of Emerging and Selected Topics in Power Electronics*, vol. 2, no. 3, pp. 691-700, Apr. 2014.
- [37] A. Hoke, A. Brissette, K. Smith *et al.*, "Electric vehicle charge optimization including effects of lithium-ion battery degradation," in *Proceedings of 2011 IEEE Vehicle Power and Propulsion Conference*, Chicago, USA, Sept. 2011, pp. 1-6.
- [38] W. Hu, G. Yen, and X. Zhang, "Multiobjective particle swarm optimization based on Pareto entropy," *Software*, vol. 25, no. 5, pp. 1025-1050, May 2014.

Hongqian Wei received the B.S. degree in electrical power engineering from Beijing Institute of Technology, Beijing, China, in 2016, where he is currently working toward a Ph.D. degree in electrical engineering. He is jointly pursuing a Ph.D. degree in the Department of Electrical Engineering at Cardiff University, Cardiff, UK. His current research interests include distributed electric vehicle control, autonomous in-wheel motor drive electric vehicles, vehicle-to-grid technology, and modern control theory.

Jun Liang received the B.S degree from Huazhong University of Science and Technology, Wuhan, China, in 1992, and M.Sc. and Ph.D. degrees from

the China Electric Power Research Institute (CEPRI), Beijing, China, in 1995 and 1998, respectively. From 2005 to 2007, he was with the University of Glamorgan, Glamorgan, UK, as a Senior Lecturer. Currently, he is a Professor at the School of Engineering, Cardiff University, Cardiff, UK. He is a Fellow of the Institution of Engineering and Technology (IET). He is the Chair of the IEEE UK and Ireland Power Electronics Chapter. His research interests include high-voltage direct current, medium-voltage direct current, flexible alternative current transmission systems, power system stability control, power electronics, and renewable power generation.

Chuanyue Li received the B.Eng. degrees in electrical and electronic engineering from Cardiff University, Cardiff, UK, and North China Electric

Power University, Beijing, China, in 2013, and the Ph.D. degree in electrical and electronic engineering from Cardiff University, in 2017. His research interests include high-voltage direct current control and protection and power electronics.

Youtong Zhang received the Ph.D. degree in power machinery and engineering from Beijing Institute of Technology, Beijing, China, in 1995. He is currently a Professor at the School of Engineering and the Director of the Low Emission Vehicles (Beijing Key Lab) Research Laboratory, Beijing Institute of Technology. His research interests include electrical engine control, new energy vehicles, and the application of power electronics in EVs/hybrid EVs.